Published in *ASCE Journal of Geotechnical and Geoenvironmental Engineering*, 139(9):1554-1566. http://dx.doi.org/10.1061/(ASCE)GT.1943-5606.0000882

Critical skirt spacing for shallow foundations under general loading

Divya S.K. MANA
Centre for Offshore Foundation Systems (M053) and ARC Centre of Excellence for Geotechnical Science and Engineering
University of Western Australia
Email: 20674905@student.uwa.edu.au

Susan GOURVENEC (corresponding author)
Centre for Offshore Foundation Systems (M053) and ARC Centre of Excellence for Geotechnical Science and Engineering
University of Western Australia
35 Stirling Highway, Crawley
Perth, WA 6009
Australia
Tel: +61 8 6488 3995
Fax: +61 8 6488 1044
Email: susan.gourvenec@uwa.edu,au

Christopher M. MARTIN
Department of Engineering Science
University of Oxford
Email: chris.martin@eng.ox.ac.uk

No. of words: 5607 (without abstract, acknowledgements and references)
No. of tables: 0
No. of figures: 23

Abstract

Finite element limit analysis is used to identify the critical internal skirt spacing for undrained failure of shallow skirted foundations under conditions of plane strain, based on the criterion that the confined soil plug should ideally displace as a rigid block, such that optimal bearing capacity is realized. General loading (vertical, horizontal and moment) is considered for foundations with skirt embedments ranging from 5% to 50% of the foundation breadth, in soil having either uniform strength or strength proportional to depth. The results explicitly identify the number of internal skirts required to ensure soil plug rigidity under arbitrary combinations of horizontal and moment loading, expressed as a function of the normalized skirt embedment and the maximum expected level of vertical loading (as a fraction of the ultimate vertical bearing capacity). It is shown that fewer internal skirts are required with increasing normalized foundation embedment, but more internal skirts are required if the soil strength increases with depth. The results also indicate the potential for a significant reduction in capacity if insufficient skirts are provided, such that plastic deformation is permitted to occur within the soil plug.

Key words: Offshore structures; Limit analysis; Shallow foundations; Failure loads

1 Introduction

Skirted shallow foundations are comprised of a main foundation base plate with relatively slender vertical plates (typically both peripheral and internal) protruding below. These 'skirts' penetrate into the seabed, with the aim of confining a block of surficial soil referred to as the soil plug. A cross-section through an idealized skirted foundation is shown in Figure 1. In order to achieve maximum capacity, sufficient internal skirts should be provided to ensure that the soil plug displaces as a rigid body during plastic failure of the foundation. If too few internal skirts are provided, failure mechanisms involving deformation within the soil plug may occur, leading to a reduction in load-carrying capacity. Figure 2 illustrates some examples of these potential 'internal mechanisms', as compared with the behavior of a corresponding solid foundation, for the simplified cases of pure vertical and pure horizontal loading. In the examples shown, deformation within the soil plug occurs when there are no internal skirts and when a single internal skirt is provided, while the provision of two (or more) internal skirts results in the same failure mechanism as that induced by the solid foundation.

Previous research has shown that for foundations with peripheral skirts only, an internal mechanism is unlikely to occur for deep skirts and a uniform profile of undrained strength with depth, but the potential is increased for shallow skirts and a high degree of strength heterogeneity (Yun and Bransby 2007, Bransby and Yun 2009, Mana et al. 2010). Although these previous works have identified the foundation configurations and soil conditions most susceptible to the development of internal mechanisms, the question of the number of internal skirts required to ensure rigid soil plug behavior –

whether for idealized cases of uniaxial loading or more realistic combinations of general loading – has not been addressed to date.

Despite the potential for plastic deformation to occur within the soil plug, skirted foundations are often treated as embedded solid foundations when assessing ultimate capacity, on the basis that sufficient internal skirts have been provided to ensure that the soil plug displaces rigidly. For example, the assumption of a solid, rigid foundation is inherent in the classical bearing capacity calculation methods presented in current recommended practices and industry guidelines (e.g. API 2000, ISO 2003). If, however, the provision of internal skirts is insufficient, the critical collapse mechanism will extend into the soil plug, resulting in a load-carrying capacity that is smaller than the anticipated design value.

This paper presents results from a comprehensive numerical investigation of the critical number of internal foundation skirts required to ensure that the soil plug confined within a skirted foundation displaces as a rigid block, thus ensuring that the maximum load-carrying capacity of the foundation can be realized.

2 Scope of study

2.1 Foundation geometry

This study considers both solid and skirted shallow foundations with embedment to breadth ratios, d/B, between 5% and 50%. The range of embedment ratio was selected to represent a range encountered in the field, for example shallow foundations for subsea systems typically lie in the range $0.05 \leq d/B \leq 0.2$ while foundations for fixed-bottom or buoyant platforms typically lie in the range $0.2 \leq d/B \leq 0.5$. For the skirted

92 foundations, the peripheral and internal skirts are modeled with a thickness to breadth
93 ratio t/B = 0.001 and are positioned with uniform spacing, s, across the foundation base
94 plate. The modeled skirt thickness ratio represents a value towards the lower end of the
95 range used in the field (e.g. Bye et al. 1995, Erbrich and Hefer 2002) and has been
96 selected to minimize the effect of the geometry of the skirts on the calculated bearing
97 capacities and failure mechanisms. A foundation with peripheral skirts only is referred
98 to as having 'zero internal skirts'. Figure 3 shows the modeled geometry and the
99 nomenclature adopted in this paper.

100 In practice, skirted foundations and/or the distribution of internal skirts may often adopt
101 a three-dimensional arrangement. Skirted foundations for gravity base structures,
102 jackets or buoyant facilities are likely to be quasi-circular or rectangular with length to
103 breadth aspect ratio L/B between 1 and 2 while subsea foundations are likely to be
104 rectangular, also with L/B between 1 and 2.

105 However, plane strain modeling is considered adequate for the purpose of this study,
106 where the focus is identifying underlying mechanisms. Failure mechanisms dominated
107 by sliding and rotation are essentially in-plane and therefore shape effects of three-
108 dimensional foundation geometry would not be expected to be significant. Failure
109 mechanisms with a significant axisymmetric component, such as vertical bearing
110 failure, would be expected to be more significantly affected by three dimensional
111 effects, although design situations with vertical load close to critical values are perhaps
112 unlikely. When considering foundations with a length to breadth aspect ratio greater
113 than 1, it should be borne in mind that the effective embedment ratio for loading acting
114 perpendicular to the long edge is defined by d/L rather than d/B, such that closer

spacing of skirts may be required along the long axis of the foundation compared with the short axis. It is probable that three-dimensional effects, if relevant, would increase the stability of the soil plug, such that a prediction of critical skirt spacing – or the minimum required number of internal skirts – based on plane strain conditions would lead to a design erring on the safe side.

2.2 Soil properties

The soil is modeled as a rigid–plastic, purely cohesive material, such that its response is defined completely in terms of the undrained shear strength, s_u. In the field, the variation of strength with depth can often be approximated with sufficient accuracy as a linear function. The degree of strength heterogeneity can then be defined in terms of the dimensionless group kB/s_{um}, where k is the gradient of the strength profile, B is the foundation breadth and s_{um} is the mudline strength intercept. In this study two limiting strength profiles are considered: uniform ($kB/s_{um} = 0$) and linearly increasing with depth from zero strength at the mudline ($kB/s_{um} = \infty$). These two cases are illustrated schematically in Figure 4.

2.3 Interface conditions

The skirted foundations are modeled as perfectly smooth, such that no shear stress can be mobilized along the foundation–soil interface (roughness factor $\alpha = 0$). This is to ensure that the capacity calculations are conservative with respect to interface strength (in practice it is more usual to assume $\alpha = 0.3$ to 0.8). The extent of the smooth interface includes all surfaces in contact with the soil: the external and internal skirt faces, the skirt tips and the underside of the foundation base plate.

The solid foundations are modeled with smooth sides ($\alpha = 0$) and fully rough bases ($\alpha = 1$). The rough base of the solid foundation is intended to be comparable with the soil-on-soil shearing surface that develops at the base of a skirted foundation, assuming sufficient internal skirts have been provided.

In all cases the foundation–soil interface is taken to be fully bonded, i.e. unlimited tensile normal stresses can be mobilized between the foundation and the soil. It is well established that negative excess pore pressures can develop between the underside of the foundation base plate and the soil plug, allowing transient uplift to be resisted (Dyvik et al. 1993, Andersen and Jostad 1999, Watson et al. 2000, Gourvenec et al. 2009, Mana et al. 2012). A 'zero-tension' interface is not considered here since, should a gap form, local drainage would take place in the vicinity of the foundation, and the duration over which the negative excess pore pressures in the soil plug could be relied upon to resist transient uplift loads would be compromised. The assumption of undrained behavior, as adopted in this study, would therefore be invalid. It is acknowledged that gapping between the foundation skirts and the adjacent soil may occur, particularly when a foundation is subjected to predominantly horizontal loading in soil with a low degree of strength heterogeneity. However, the potential for gapping is a separate consideration in the design process.

2.4 Loading

The solid and skirted foundations are modeled as discrete rigid bodies with a single load reference point located on the centerline of the foundation at mudline level. The sign convention for combined vertical, horizontal and moment loading (V, H, M) is defined in Figure 5.

Figure 6 shows the procedure used to establish failure envelopes for combined loading. Initial analyses involving pure vertical loading are used to identify the vertical bearing capacity, V_{ult}, of each foundation. Ultimate limit states for combined loading are then identified by conducting radial probes in M/B:H space at constant V. These probes are defined by an angle θ (see Figure 6) and are applied at 5º intervals from 0º to 180º. Various levels of vertical load are considered, relative to the uniaxial vertical capacity of the corresponding solid foundation: V/V_{ult} = 0, 0.1, 0.25, 0.5 and 0.75. For each probe, lower and upper bound collapse loads are computed as described in the following section. The respective solution points are joined as shown in Figure 6 to give lower and upper bound failure envelopes for each plane of constant V/V_{ult}.

The soil and the foundations are all modeled as weightless materials, thus ensuring that geostatic equilibrium is automatically satisfied at the start of each analysis. When applying these results in practice, the total weight of the foundation (minus the total weight of displaced soil) should be included as part of the applied vertical force, V.

3 Finite element limit analysis

All analyses were performed using OxLim, a finite element limit analysis (FELA) program developed at Oxford University. FELA differs from conventional finite element analysis in that it implements the classical bound theorems of limit analysis, rather than computing an approximate plastic collapse load that is approached incrementally. With FELA it is usual to compute both lower bound and upper bound plasticity solutions for a given problem, thus bracketing the range in which the exact collapse load must lie. Background information about the FELA method and its

historical development can be found in the papers by Makrodimopoulos & Martin (2006, 2007) which deal with lower bound FELA and upper bound FELA respectively. Both of these papers contain extensive reviews of the relevant literature, with an emphasis on applications of FELA to geotechnical problems.

OxLim implements various calculation methods that are described in detail by Makrodimopoulos and Martin (2006, 2007, 2008). The program also uses a simple strategy for adaptive mesh refinement (Martin 2011) that facilitates rapid convergence of the lower and upper bound solutions. At each stage of the refinement process, which is fully automatic, lower and upper bounds are computed using the same mesh. The current version of OxLim relies on two key pieces of software by others: MOSEK (MOSEK ApS 2010) for optimization and Triangle (Shewchuk 2002) for unstructured triangular mesh generation.

Essentially, each lower bound solution involves optimization of a stress field that satisfies equilibrium but does not exceed the shear strength of either the soil or the foundation–soil interface. Each upper bound solution involves optimization of a velocity field that is compatible with the motion of the footing (which has three degrees of freedom in plane strain) and generates a strain field that satisfies the associated flow rule. The finite elements employed in OxLim are as follows: three-noded triangles (linear interpolation of stress) for the lower bound analyses, and six-noded triangles (quadratic interpolation of velocity) for the upper bound analyses. Further details are given in the papers by Makrodimopoulos and Martin (2006, 2007). For the purely cohesive soil considered in this paper, enforcement of the associated flow rule in the

upper bound analyses is achieved by constraining the volumetric strain to be zero throughout the soil, and the normal displacement jump to be zero on all interfaces.

In the present OxLim analyses the solid and skirted foundations were 'wished in place', with no attempt to account for the surface heave that would occur during continuous penetration from the surface. The extent of the modeled soil domain (width × depth) was 4B × 2B for all the analyses except for pure vertical loading (6B × 2B), which was comfortably sufficient to contain the plastically deforming region for all embedment ratios and load combinations. The initial mesh sizing was an iterative process where the domain was defined, the analysis run and the domain was extended and the analysis re-run if the mechanism was impacted by the boundaries of the domain. The target element size (triangle side length) for generation of the initial mesh was 0.5B for the vertical loading cases and 0.3B for all other analyses, which is 0.1 times the average bounding box dimension. In each OxLim analysis, several cycles of automated adaptive mesh refinement (typically two or three) were performed until the lower and upper bound solutions bracketed the exact collapse load to within ±1%, i.e., until the percentage bracketing error, defined as (UB – LB) / (UB + LB) × 100, was smaller than 1%. Although this level of bracketing can readily be achieved for undrained bearing capacity problems, it is not worthwhile seeking even better precision because in practice the uncertainty associated with selection of the design shear strength profile is inevitably much greater.

4 Results

All results are presented in terms of normalized quantities. The geometric characteristics of the foundations are defined by the embedment ratio, d/B, and the skirt spacing ratio, s/B (see Figure 3). The bearing capacity failure envelopes, or interaction diagrams, are presented in terms of the dimensionless loads V/Bs_u, H/Bs_u and M/B^2s_u (for uniform strength) or V/B^2k, H/B^2k and M/B^3k (for strength proportional to depth). The one exception is that the vertical bearing capacities in Figure 8b are normalized by the local strength at skirt tip level, $s_{u0} = kd$, in order to illustrate more clearly the effect of the number of internal skirts on the familiar bearing capacity factor N_c.

4.1 Validation

The first validation exercise was to confirm that OxLim produced correct results for the vertical bearing capacity of a surface strip footing on soil with uniform strength ($kB/s_{um} = 0$) and strength proportional to depth ($kB/s_{um} = \infty$). In both cases exact analytical solutions are available, $V_{ult}/Bs_u = 2 + \pi$ (Prandtl 1921) and $V_{ult}/B^2k = 1/4$ (Davis and Booker 1973), and both results are independent of the footing roughness. As expected, the lower and upper bound solutions obtained from OxLim were found to bracket each of these exact solutions to within the target bracketing precision of ±1%.

In terms of validation against established (albeit numerical) results, Figure 7 compares some combined loading failure envelopes obtained using Oxlim with those obtained using the commercial finite element software Abaqus (Dassault Systèmes 2009) given by Gourvenec and Barnett (2011). The problem considered is the basic case of a rough strip footing on the surface of a soil deposit with uniform strength. Figure 7 shows that

there is good overall agreement between the two methods. Furthermore, for each value of V/V_{ult}, the lower and upper bound failure envelopes from OxLim lie very close together, demonstrating that even for general loading conditions, tight numerical bracketing of the exact solution was achieved using FELA.

4.2 Vertical loading

Figure 8 compares vertical bearing capacity factors for solid and skirted foundations as a function of embedment ratio, for both uniform strength ($kB/s_{um} = 0$) and strength proportional to depth ($kB/s_{um} = \infty$). In the latter case, the vertical capacity V_{ult} is normalized with respect to s_{u0}, the strength at depth d, as this best illustrates the variation of bearing capacity as a function of the number of internal skirts at low d/B, and the convergence of bearing capacity with increasing d/B. Also with respect to Figure 8b, it should be noted that in the reduction in bearing capacity *factor* with increasing embedment ratio is an effect of normalization by an ever-increasing strength at skirt tip level; the actual bearing capacity V_{ult} increases with d/B. In Figure 8 average values of the lower and upper bound solutions from OxLim are shown.

Figure 8a shows that in uniform soil, the vertical bearing capacity of a foundation with peripheral skirts only (i.e. zero internal skirts) is equal to that of a solid embedded foundation, indicating that the soil plug displaces rigidly even without the provision of internal skirts. By contrast, Figure 8b shows that in soil with strength proportional to depth, the bearing capacity is markedly affected by the absence or provision of internal skirts, particularly for embedment ratios $d/B < 0.3$.

The trends of the bearing capacity factors presented in Figure 8 are reflected in the mechanisms accompanying failure. For soil with uniform strength, the solid and externally skirted foundations exhibit identical mechanisms over the full range of embedment ratios considered ($0.05 \leq d/B \leq 0.5$). Figure 9 illustrates these mechanisms for selected embedment ratios of $d/B = 0.1$ and 0.5. The similarity of the mechanisms for the solid and skirted foundations echoes the similarity of the bearing capacity factors. For soil with strength proportional to depth, the difference in bearing capacity factor (as seen in Figure 8b, $d/B < 0.3$) arises from a difference in failure mechanism. Significant plastic deformation can now take place within the soil plug, particularly at low embedment ratios, as illustrated for an example case, $d/B = 0.1$, in Figure 10. It is however possible for the soil plug of a skirted foundation in soil with a high degree of strength heterogeneity to behave rigidly in the absence of internal skirts, provided the embedment is sufficient. This is clear from the mechanisms in Figure 11 ($kB/s_{um} = \infty$ and $d/B = 0.5$) and is reflected in the convergence of the various curves in Figure 8b for embedment ratios $d/B > 0.3$.

The results presented in Figure 8 to 11 are consistent with existing theoretical solutions. Broadly speaking, for a skirted foundation, an internal failure mechanism would not be expected to develop when a Prandtl-type mechanism governs failure of the corresponding solid foundation, but it would be expected when a Hill-type mechanism governs failure. (Prandtl- and Hill-type mechanisms are illustrated schematically in Figure 12) For surface foundations ($d/B = 0$) it is well established that a Hill-type mechanism governs failure of smooth footings and becomes critical for rough footings when the degree of strength heterogeneity, quantified by the dimensionless group kB/s_{um}, reaches a threshold of approximately 1 (Kusakabe et al. 1986). A similar trend

has been noted for embedded solid foundations, with a Hill-type mechanism being critical for smooth-based embedded foundations and having the potential to become critical for rough-based embedded foundations, particularly in the presence of a strength heterogeneity ratio larger than 1 or 2 (Martin and Randolph 2001). Because skirted foundations are essentially rough-based due to the soil-on-soil interface at skirt tip level, a Prandtl-type mechanism would be expected to govern vertical bearing capacity failure in a soil having uniform strength with depth, while a Hill-type mechanism would be expected in a deposit having a highly heterogeneous strength profile – as was observed in the FELA analyses undertaken for this study.

4.3 General loading

Failure envelopes in normalized H-M load space were calculated in selected planes of constant V, expressed as a percentage of the uniaxial vertical capacity, V_{ult}, of a corresponding solid foundation. Failure envelopes for a solid foundation, and for skirted foundations with up to eight internal skirts, were calculated for all combinations of the following parameters:

- embedment ratio d/B = 0.05, 0.1, 0.2, 0.3 and 0.5
- shear strength gradient kB/s_{um} = 0 and ∞
- vertical load level V/V_{ult} = 0, 0.1, 0.25, 0.5 and 0.75

In each case, OxLim was used to perform a series of radial probes as shown in Figure 6, resulting in both lower bound and upper bound failure envelopes. For clarity, however, only the upper bound envelopes are plotted in the figures below.

Examples of the calculated failure envelopes are illustrated in Figure 13 to 16 for two selected embedment ratios (d/B = 0.1 and 0.5), both strength profiles (kB/s_{um} = 0 and ∞)

314 and three selected vertical load levels (V/V_{ult} = 0, 0.5 and 0.75). The interpreted results
315 for the whole study are summarized in Figure 22and 23, and are discussed in detail in
316 the section 'Design Recommendations'.

317 In Figure 13 to 16 generally, the innermost failure envelope corresponds to a foundation
318 with peripheral skirts only. The addition of internal skirts leads to an increase in load-
319 carrying capacity, which is reflected in expansion of the H-M failure envelope on each
320 plane of constant V. The outermost failure envelope corresponds to the rough-based
321 solid foundation that defines the optimum, maximum load-carrying capacity (and is in
322 most cases coincident with the failure envelope for a skirted foundation with sufficient
323 internal skirts).

324 Figure 13 shows failure envelopes for a foundation with shallow skirts (d/B = 0.1) in
325 uniform soil (kB/s_{um} = 0). In the absence of vertical load (V/V_{ult} = 0) a single internal
326 skirt is sufficient to ensure that the soil plug displaces rigidly under any combination of
327 horizontal and moment load, such that optimal capacity is achieved. With increasing
328 vertical load, additional internal skirts are required to ensure plug rigidity under all
329 combinations of H and M. When V/V_{ult} = 0.75, loading ratios M/B:H ≈ 0.3 to 2.0 are
330 critical – i.e. they require the largest number of internal skirts before reaching the
331 maximum capacity. Strictly speaking, the optimal configuration requires five internal
332 skirts, though little improvement in capacity is achieved with more than two skirts.
333 Figure 14 shows corresponding failure envelopes for a foundation with deeper skirts
334 (d/B = 0.5) in soil with uniform strength. In this case low vertical loads are critical,
335 requiring one internal skirt to ensure soil plug rigidity, while under higher vertical loads

the optimal solid foundation capacity is achieved for all directions of loading in H-M space, even if no internal skirts are provided.

Figure 15 and 16 show that when the soil strength is proportional to depth ($kB/s_{um} = \infty$), more internal skirts are required, particularly when the skirt embedment ratio is low, as in Figure 15. This would be expected since with this type of strength profile, there is a strong tendency for the failure mechanism to propagate into the softer, near-surface soil. In fact, Figure 15 shows that six or more internal skirts are required to ensure soil plug rigidity for a foundation with d/B = 0.1 in soil with strength proportional to depth – twice as many as are required with the same embedment ratio in a deposit with uniform strength (cf. Figure 13). When the skirts are longer, Figure 16 (for d/B = 0.5) shows that failure to provide any internal skirts leads to a significant loss of capacity with respect to the optimum. However, there is little benefit in providing more than one internal skirt, since this is sufficient to achieve maximum capacity for nearly all loading directions in H-M space, at all levels of vertical load.

It is noteworthy that optimal foundation capacity of a skirted foundation may fall short of the capacity of a rough-based solid foundation with the same embedment ratio, particularly for shallow embedment in soil with a high degree of strength heterogeneity. That is, addition of further skirts does not lead to an incremental increase in capacity and the maximum capacity obtained is less than that for an equivalent rough-based solid foundation. In the case of zero mudline strength ($kB/s_{um} = \infty$) the failure mechanism at skirt tip level may be affected by the potential zero-strength failure plane on the underside of the foundation base plate; a smooth foundation–soil interface would have the same effect in soil with a non-zero mudline strength. In this study, a smooth skirted

foundation gave inferior V-H-M capacity, compared with a smooth-sided rough-based solid foundation of equal embedment ratio, when d/B = 0.05, i.e. convergence of the failure envelopes of the skirted foundations with n and n + 1 internal skirts occurred at a lower ultimate limit state than that achieved by the solid foundation (Figure 17). However, when the embedment ratio exceeds a critical value ($0.05 < d/B \leq 0.1$ in this study) the effect of soil-on-soil shearing at skirt tip level becomes sufficiently remote from the zero-strength underside of the foundation base plate, and equal bearing capacity can be mobilized by a smooth skirted foundation and a smooth-sided rough-based solid foundation. In the limit of an infinite number of smooth-sided, smooth-tipped internal skirts being provided, the capacity of a skirted foundation would tend towards that of a smooth-based solid foundation. In practice, with normalized skirt thicknesses rarely exceeding t/B = 0.01, the ratio of total skirt tip area to overall foundation area would typically be less than 5%.

Failure envelopes for combined loading, such as those in Figure 13 to 16, show that the number of internal skirts is always critical for 'positive' combinations of H-M loading, i.e. H and M both acting in their positive directions (according to the sign convention defined in Figure 5). This is of course the case in nearly all practical situations, with moment loading arising from horizontal loads acting on the superstructure at various lever arms above the mudline. Furthermore, the number of internal skirts is critical mostly at high levels of vertical load ($V/V_{ult} = 0.5$ or greater), indicating potential efficiencies if the applied vertical loads are known to be limited – as is often the case for skirted mat foundations for subsea structures.

The failure mechanisms occurring under general loading confirm the trends observed in the failure envelopes. Figure 18 to 21 illustrate failure mechanisms for selected V-H-M load combinations, considering foundations with embedment ratios d/B = 0.1 and 0.5, and both of the strength profiles considered. In each figure, the solid foundation is compared with a series of skirted foundations, beginning with the externally skirted case (zero internal skirts) and showing the transition in failure mechanism as internal skirts are added, up to the point where effective rigidity of the soil plug is achieved and the failure mechanism is essentially identical to that of the solid foundation. Note that the load combinations corresponding to the mechanisms in Figure 18 to 21 are cross-referenced in the failure envelope plots in Figure 13 to 16 respectively.

4.4 Design recommendation

Figure 22 is a summary plot showing the number of internal skirts necessary for a plane strain skirted foundation to displace with a rigid soil plug, and thus achieve maximum capacity under general V-H-M loading. The critical number of skirts is identified either by convergence of the H-M failure envelopes of skirted foundations with n and n +1 internal skirts, or by convergence of the H-M failure envelope of the skirted foundation with that of the solid foundation, at every vertical load level. The number of internal skirts required for ‘practical’ convergence of the failure envelopes, rather than strict coincidence of the failure envelopes, was determined with a certain amount of engineering discretion. For example (as mentioned earlier) considering the results in Figure 13, strictly five internal skirts are required to achieve coincidence of the failure envelope of the skirted foundation with that of the solid foundation, although negligible

403 improvement in capacity is achieved with more than two skirts. In this case, the critical
404 number of internal skirts is taken as two.

405 The solid lines in Figure 22 indicate a linear interpolation between the critical (i.e. the
406 minimum) number of internal skirts required to mobilize maximum V-H-M capacity for
407 each of the embedment ratios considered in this study. In practice, interpolated values of
408 the critical number of skirts for intermediate embedment ratios should be rounded up in
409 order to err on the safe side – as indicated by the broken lines in Figure 22.

410 It is clear from Figure 22 that more skirts are required for low skirt embedment ratios
411 and for soils with a high degree of strength heterogeneity. In many cases, more than
412 twice as many internal skirts are required in soil with strength proportional to depth
413 ($kB/s_{um} = \infty$) compared with uniform soil ($kB/s_{um} = 0$) across the range of embedment
414 ratios considered in this study.

415 Figure 22 also reveals a non-linear relationship between the required number of internal
416 skirts and the embedment ratio, with a higher rate of change at low embedment ratios.
417 For $d/B > 0.2$, the required number of internal skirts begins to stabilize, particularly in
418 the soil with uniform strength. A continued reduction in the required number of internal
419 skirts, and a diminishing effect on bearing capacity of the development of an internal
420 mechanism, is clearly to be expected with increasing embedment ratio. However, there
421 is no evidence here to suggest that increasing the embedment ratio will eventually
422 guarantee soil plug rigidity without the provision of internal skirts. Indeed, it has been
423 noted elsewhere that failure mechanisms for suction caissons, with typical length to
424 diameter ratios in excess of three, can involve an ‘inverted scoop’ mechanism at the

425 base of the soil plug if the center of rotation is located beneath the toe of the caisson
426 (Randolph and House 2002).

427 As discussed above, Figure 22 defines the required number of internal skirts for plug
428 soil rigidity under *any* combination of V-H-M loading, and efficiencies may be realized
429 if limited vertical loads can be relied upon in-service. In practice, the design of many
430 subsea foundations is dominated by the H and M load components, and the design
431 vertical load, V, is less than 25% of the ultimate vertical capacity, V_{ult}. Figure 23 shows
432 the required number of internal skirts needed to achieve maximum H-M capacity under
433 various levels of vertical load, V/V_{ult}. This indicates that fewer skirts are often sufficient
434 if the vertical load is limited. In the case of soil with strength proportional to depth,
435 Figure 23b, a reduction in the required number of internal skirts is achieved over the full
436 range of embedment ratios. For uniform soil, Figure 23 a, efficiencies are only realized
437 for low embedment ratios ($d/B < 0.2$). This is because efficiencies of this type can only
438 be achieved for cases where high vertical loading provides the critical case (in terms of
439 the number of skirts required), e.g. in Figure 13. Limiting the applied vertical load will
440 not lead to a reduction in the required number of internal skirts if the critical case is
441 associated with low vertical load, e.g. in Figure 14.

442 The efficiencies available from limiting the vertical load level are relatively modest,
443 even when $kB/s_{um} = \infty$, with one or at most two internal skirts being saved (although at
444 high embedment ratios this is a reduction by half). This indicates that the required
445 number of internal skirts is governed by the H and M components of loading, rather
446 than the V component. As such, explicit consideration of the horizontal and moment
447 loading applied to a skirted foundation should form an essential part of the design.

4.5 Practical considerations

The curves presented in Figure 23 provide a practical guideline for determining the minimum number of internal skirts. However, the data should be treated with caution and considered with regard to the following points:

- These results have been derived for idealized material characteristics, foundation geometries and interface conditions. In practice, a variety of other factors (e.g. strength anisotropy) may affect the maximum load-carrying capacity, and there may also be installation problems (e.g. tilting, or failure to achieve full skirt penetration) that affect the effective embedment depth achieved.
- The present investigation is restricted to an idealized two-dimensional (plane strain) cross-section through a skirted foundation. In the case of a square, circular or rectangular skirted foundation, significant three-dimensional effects may be present in the failure mechanisms under various load combinations, and the results presented in Figure 22 and 23 would be expected to provide a conservative prediction of the required number of internal skirts.
- In reality, a foundation with very short skirts placed on soil with low mudline strength will tend to settle until sufficient bearing capacity is achieved, resulting in a higher effective embedment and thus a reduction in the required number of internal skirts. For example, a foundation with d/B = 0.05 placed on a soil with (near) zero mudline strength may not require the full complement of five or six internal skirts as indicated by the results presented in Figure 22 and 23. Conversely, unanticipated soil plug heave during installation, or scour around the foundation, may reduce the effective embedment depth, leading to insufficient internal skirts being provided to ensure rigidity of the soil plug, and an associated reduction in foundation capacity.

5 Concluding remarks

This paper has presented results from an extensive numerical study, carried out using finite element limit analysis, of the undrained capacity of shallow skirted foundations under general V-H-M loading. In particular, the focus has been on the critical number of internal foundation skirts necessary to ensure that the soil plug confined by a skirted foundation displaces rigidly, such that maximum foundation load-carrying capacity (equivalent to that of a corresponding solid foundation) can be mobilized.

The critical number of internal skirts has been identified for skirt embedments ranging from 5% to 50% of the foundation breadth, considering soils with both uniform strength and strength proportional to depth (representing the extremes of the generic linearly varying strength profile characterized by the dimensionless parameter kB/s_{um}). The results indicate that the skirt embedment, the degree of strength heterogeneity and the level of applied vertical load all have significant influences on the number of internal skirts required. The critical number of internal skirts has been quantified by constructing numerous V-H-M failure envelopes, and by studying the corresponding failure mechanisms. The overall findings have been summarized in graphical form (Figure 22 and 23) as a function of the key variables.

The results presented provide practical guidance on the minimum number of foundation skirts that should be provided to prevent an internal mechanism developing within the soil plug, thereby allowing the optimum load carrying capacity of a skirted foundation to be realized. Further research is required to extend these findings to general loading of skirted foundations with three-dimensional geometries.

ACKNOWLEDGEMENTS

The work described in this Paper forms part of the activities of the Special Research Centre for Offshore Foundation Systems (COFS), currently supported as a node of the Australian Research Council Centre of Excellence for Geotechnical Science and Engineering. The work presented in this paper was supported through ARC grant DP0988904. This support is gratefully acknowledged.

The work was carried out during an academic visit of the first and second authors to the Department of Engineering Science, University of Oxford, UK. The support of the Department of Engineering Science and the University of Oxford is gratefully acknowledged. MatLab scripting advice from Prof. David White is also gratefully acknowledged.

REFERENCES

API (2000). *Recommended practice for planning, designing and constructing fixed offshore platforms - working stress design*. API RP-2A, American Petroleum Institute, Washington, USA.

Andersen, K.H. and Jostad, H.P. (1999). "Foundation design of skirted foundations and anchors in clay." *Proc. Annual Offshore Technology Conf.*, Houston, Paper OTC 10824.

Bransby, M.F. and Yun, G. (2009). "The undrained capacity of skirted strip foundations under combined loading." *Géotechnique* 59(2), 115-125.

Bye, A., Erbrich, C., Rognlien, B. and Tjelta, T.I. (1995). "Geotechnical design of bucket foundations." *Proc. Annual Offshore Technology Conf.*, Houston, Paper OTC 7793.

Dassault Systèmes (2009). *Abaqus analysis users' manual*. Simulia Corp., Providence, RI, USA.

Davis, E.H. and Booker, J.R. (1973). "The effect of increasing strength with depth on the bearing capacity of clays." *Géotechnique* 23(4), 551-563.

Dyvik, R., Andersen, K.H., Hansen, S.B. and Christophersen, H.P. (1993). "Field tests of anchors in clay." I: Description. *J. Geotech. Engng., ASCE* 199(10), 1515-1531.

Erbrich, C. and Hefer, P. (2002). "Installation of the Laminaria suction piles – a case history." *Proc. Annual Offshore Technology Conf.*, Houston, Paper OTC 14240.

Gourvenec, S. and Barnett, S. (2011). "Undrained failure envelope for skirted foundations under general loading." *Géotechnique* 61(3), 263-270.

Gourvenec, S., Acosta-Martinez, H.E. and Randolph, M.F. (2009). "Experimental study of uplift resistance of shallow skirted foundations in clay under concentric transient and sustained loading." *Géotechnique* 59(6), 525-537.

ISO (2003). *Petroleum and natural gas industries – Specific requirements for offshore structures – Part 4: Geotechnical and foundation design considerations*. ISO 19901-4:2003, International Organization for Standardization.

Kusakabe, O. Suzuke, H. and Nakase, A. (1986). "An upper bound calculation on bearing capacity of a circular footing on a non-homogeneous clay." *Soils and Foundations* 26(3), 143-148.

Makrodimopoulos, A. and Martin, C.M. (2006). "Lower bound limit analysis of cohesive-frictional materials using second-order cone programming." *International Journal for Numerical Methods in Engineering* 66(4), 604-634.

Makrodimopoulos, A. and Martin, C.M. (2007). "Upper bound limit analysis using simplex strain elements and second-order cone programming." *International Journal for Numerical and Analytical Methods in Geomechanics*31(6), 835-865.

Makrodimopoulos, A. and Martin, C.M. (2008). "Upper bound limit analysis using discontinuous quadratic displacement fields." *Communications in Numerical Methods in Engineering* 24(11), 911-927.

Mana, D.S.K., Gourvenec, S. and Randolph, M.F. (2010). "A numerical study of the vertical bearing capacity of skirted foundations." *Proc. 2nd Int. Symp. Front. Off. Geotech.* (ISFOG), Perth, 433-438.

Mana, D.S.K., Gourvenec, S., Randolph, M.F. and Hossain, M.S. (2012). "Failure mechanisms of skirted foundations in uplift and compression." *International Journal of Physical Modelling in Geotechnics* 12(2), 47-62.

Martin, C.M. and Randolph, M.F. (2001). "Applications of the lower and upper bound theorems of plasticity to collapse of circular foundations." *Proc. 10th Int. Conf. Int. Assoc. Comp. Meth. Adv. Geomech. (IACMAG)*, Tucson, 1417-1428.

Martin, C.M. (2011). "The use of adaptive finite element limit analysis to reveal slip-line fields." *Geotechnique Letters* 1, 23-29.

552 MOSEK ApS (2010). *The MOSEK optimization tools manual, Version 5*. Available online at
553 www.mosek.com.

554 Prandtl, L. (1921). "Eindringungsfestigkeit und festigkeit von schneiden." *Angew. Math. U. Mech* 1(15).

555 Randolph M.F. and House A.R. (2002). "Analysis of suction caisson capacity in clay." *Proc. Annual*
556 *Offshore Technology Conf.*, Houston, Paper OTC 14236.

557 Shewchuk, J.R. (2002). "Delaunay refinement algorithms for triangular mesh generation." Computational
558 Geometry 22(1-3), 21-74.

559 Watson, P.G., Randolph, M.F. and Bransby, M.F. (2000). "Combined lateral and vertical loading of
560 caisson foundations." *Proc. Annual Offshore Technology Conf.*, Houston, Paper OTC 12195.

561 Yun, G. and Bransby, M.F. (2007). "The undrained vertical bearing capacity of skirted foundations."
562 *Soils and Foundations* 47(3), 493-505.

563

FIGURE CAPTIONS

Figure 1 Characteristics of an idealized skirted foundation

Figure 2. Examples of failure mechanisms of solid and skirted shallow foundations under (a) pure vertical load and (b) pure horizontal load

Figure 3 Definition of terminology to describe solid and skirted foundations

Figure 4 Definition of soil strength profiles

Figure 5 Sign convention and nomenclature

Figure 6 Load probes and definition of failure envelopes

Figure 7 Comparison of V-H-M failure envelopes predicted with OxLim and Abaqus: rough-based surface strip foundation on a deposit with uniform shear strength

Figure 8 Vertical bearing capacity of solid and skirted foundations for (a) $kB/s_{um} = 0$ and (b) $kB/s_{um} = \infty$

Figure 9 Soil velocity vectors accompanying vertical bearing failure of solid and externally skirted foundations for $kB/s_{um} = 0$. Examples showing (a) $d/B = 0.1$ and (b) $d/B = 0.5$

Figure 10 Soil velocity vectors accompanying vertical bearing failure of solid and skirted foundations for $kB/s_{um} = \infty$ and low embedment ratio, $d/B = 0.1$

Figure 11 Soil velocity vectors accompanying vertical bearing failure of solid and externally skirted foundations for $kB/s_{um} = \infty$ and high embedment ratio, $d/B = 0.5$

Figure 12 Hill- and Prandtl-type failure mechanisms for a shallow foundation under pure vertical load

Figure 13 Failure envelopes for $kB/s_{um} = 0$ and $d/B = 0.1$

Figure 14 Failure envelopes for $kB/s_{um} = 0$ and $d/B = 0.5$

Figure 15 Failure envelopes for $kB/s_{um} = \infty$ and $d/B = 0.1$

Figure 16 Failure envelopes for $kB/s_{um} = \infty$ and d/B = 0.5

Figure 17 Failure envelope for $kB/s_{um} = \infty$ and d/B = 0.05

Figure 18 Soil velocity vectors at failure for $kB/s_{um} = 0$ and d/B = 0.1; loading V = 0, M/B:H = 0.577

Figure 19 Soil velocity vectors at failure for $kB/s_{um} = 0$ and d/B = 0.5; loading V = 0, M/B:H = 0.577

Figure 20 Soil velocity vectors at failure for $kB/s_{um} = \infty$ and d/B = 0.1; loading V = 0.75Vult, M/B:H = -1

Figure 21 Soil velocity vectors at failure for $kB/s_{um} = \infty$ and d/B = 0.5; loading V = 0.75Vult, M/B:H = 1

Figure 22 Number of internal foundation skirts required to mobilize maximum V-H-M capacity

Figure 23 Number of internal foundation skirts required to mobilize maximum H-M capacity under various levels of vertical load for (a) $kB/s_{um} = 0$ and (b) $kB/_{sum} = \infty$

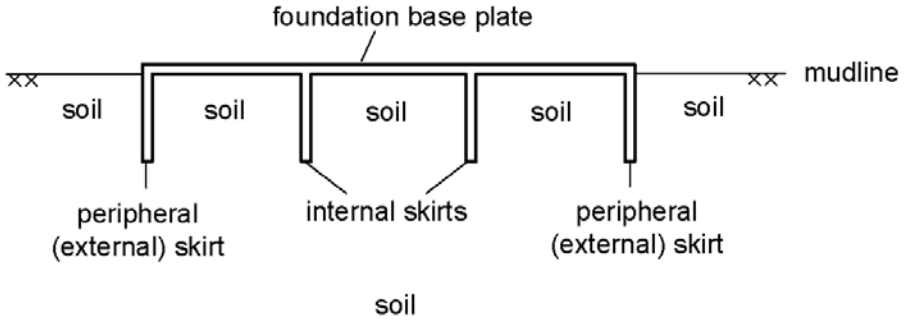

Figure 1

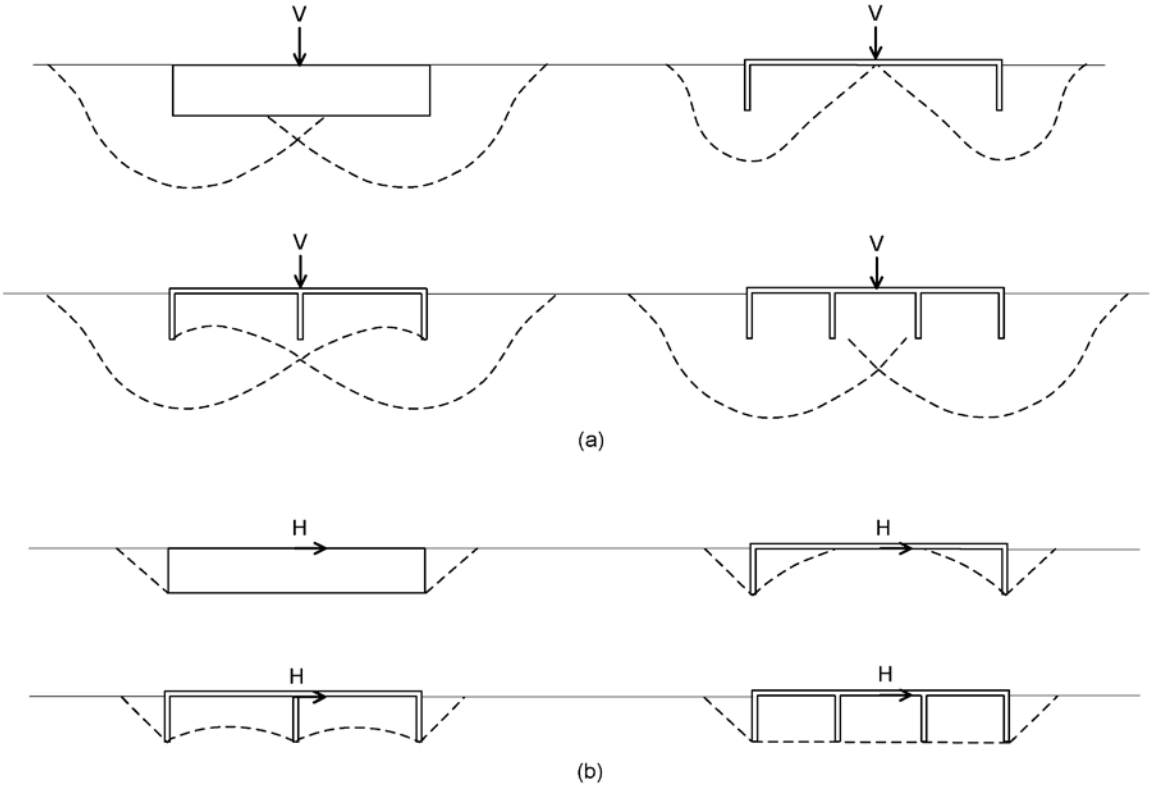

Figure 2

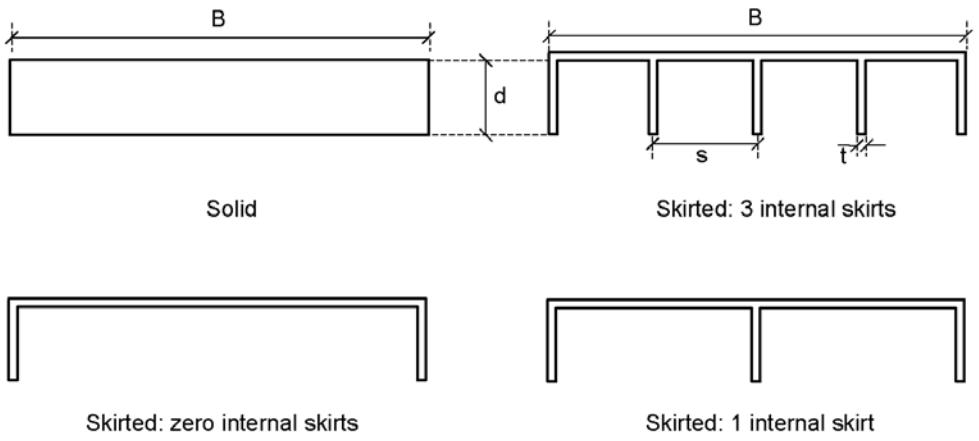

Figure 3

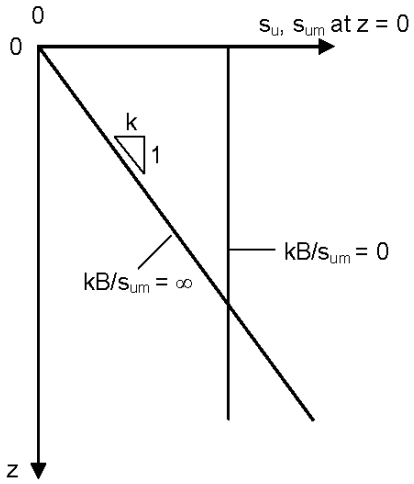

Figure 4

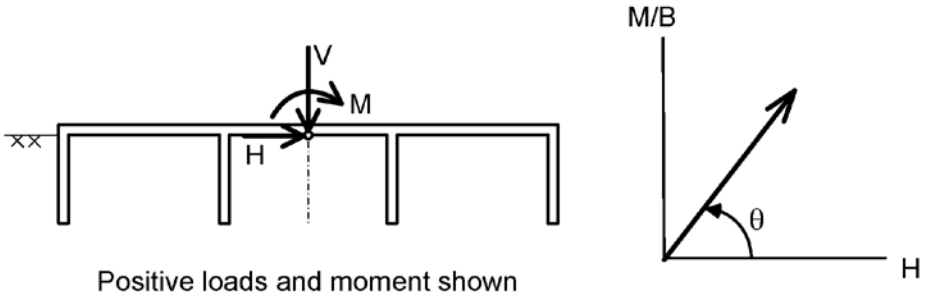

Figure 5

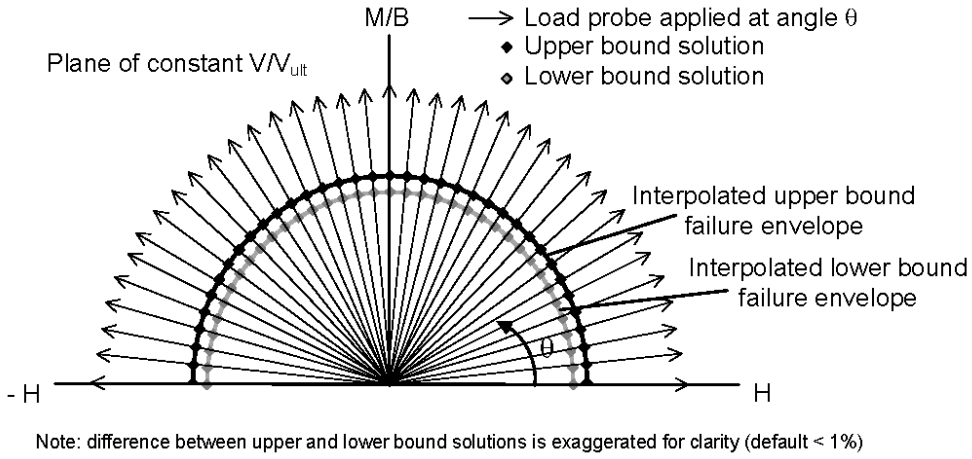

Figure 6

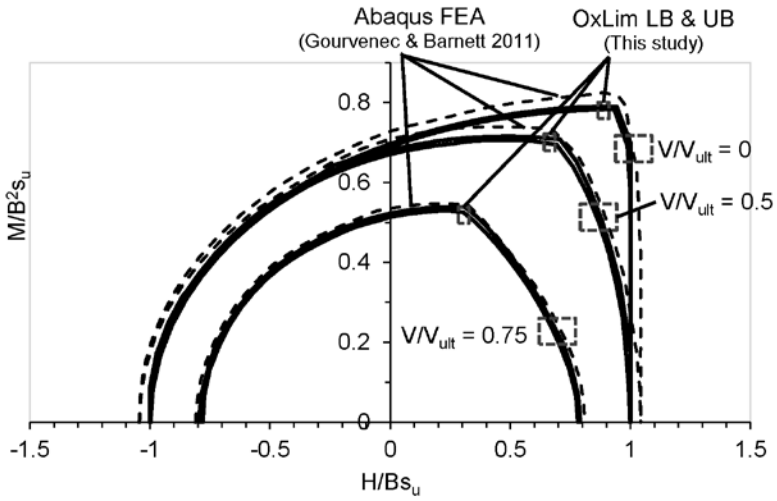

Figure 7

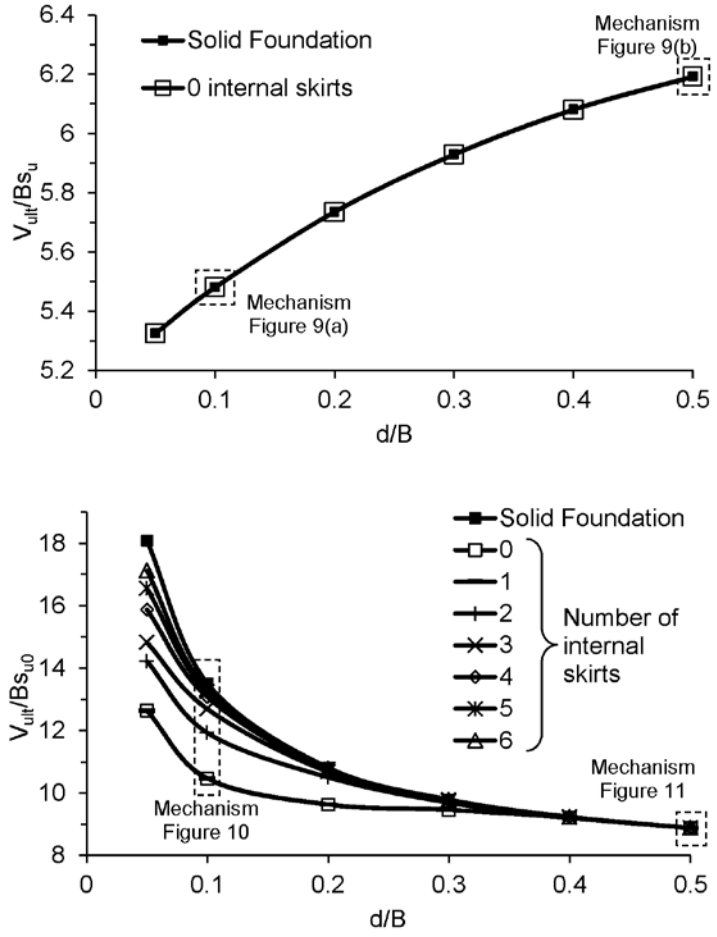

Figure 8

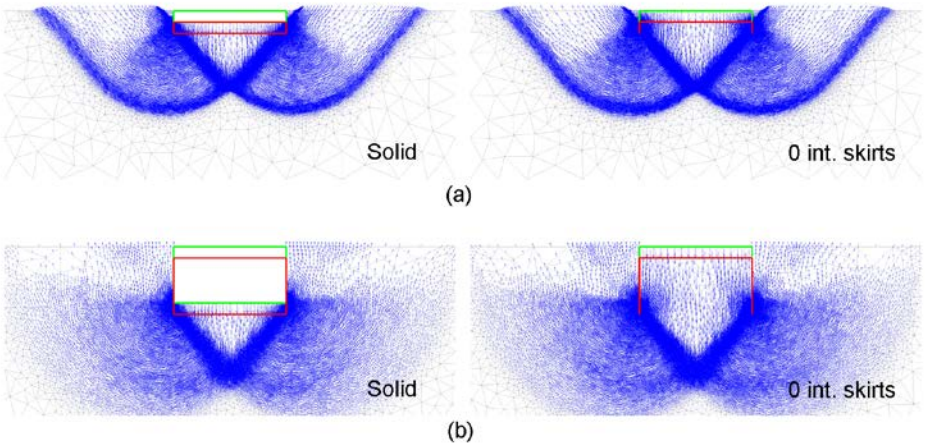

Figure 9

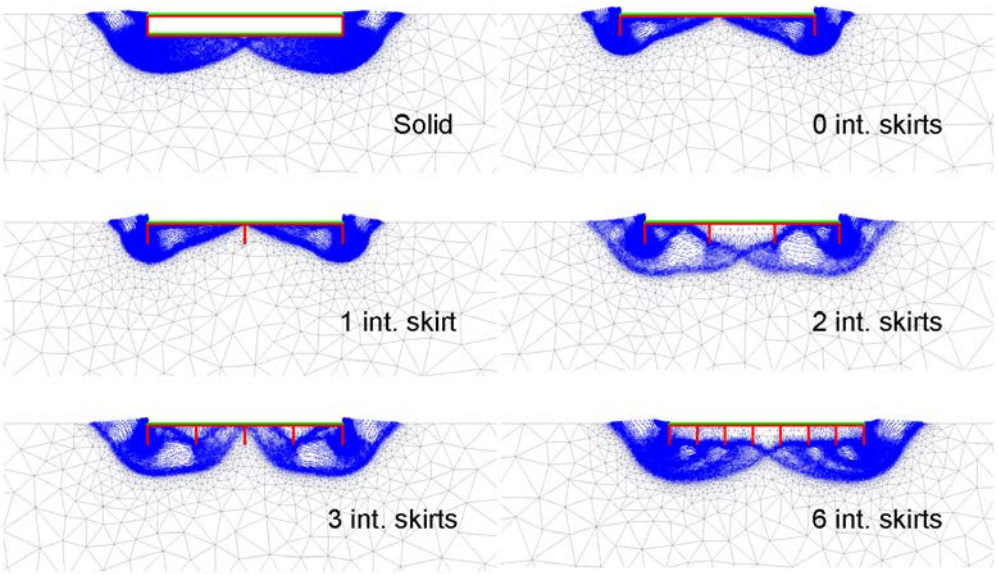

Figure 10

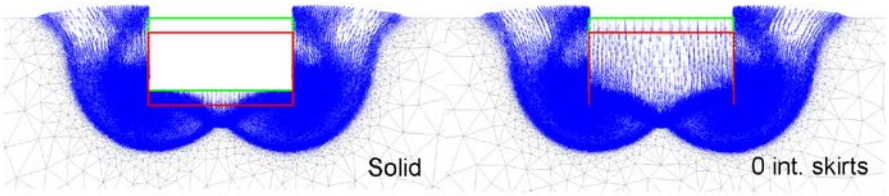

Figure 11

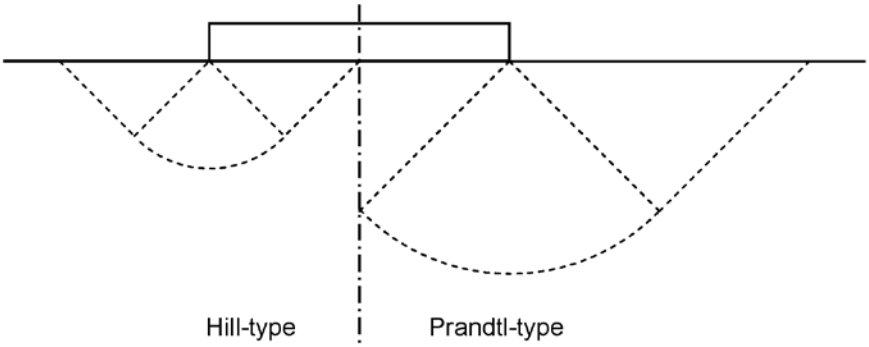

Figure 12

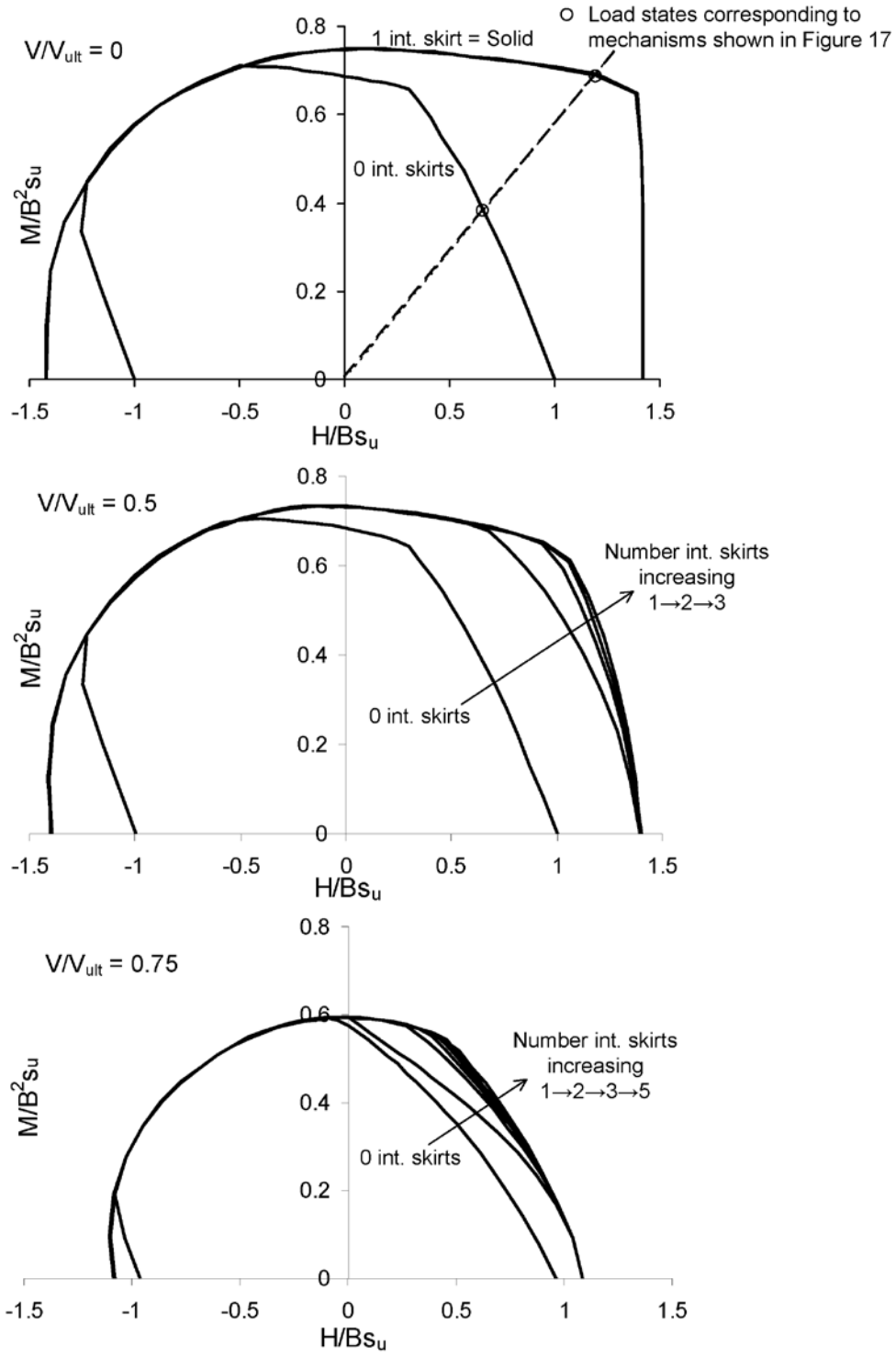
V/Vult = 0
1 int. skirt = Solid
Load states corresponding to mechanisms shown in Figure 17
0 int. skirts
M/B2su
H/Bsu
V/Vult = 0.5
Number int. skirts increasing 1→2→3
0 int. skirts
M/B2su
H/Bsu
V/Vult = 0.75
Number int. skirts increasing 1→2→3→5
0 int. skirts
M/B2su
H/Bsu

Figure 13

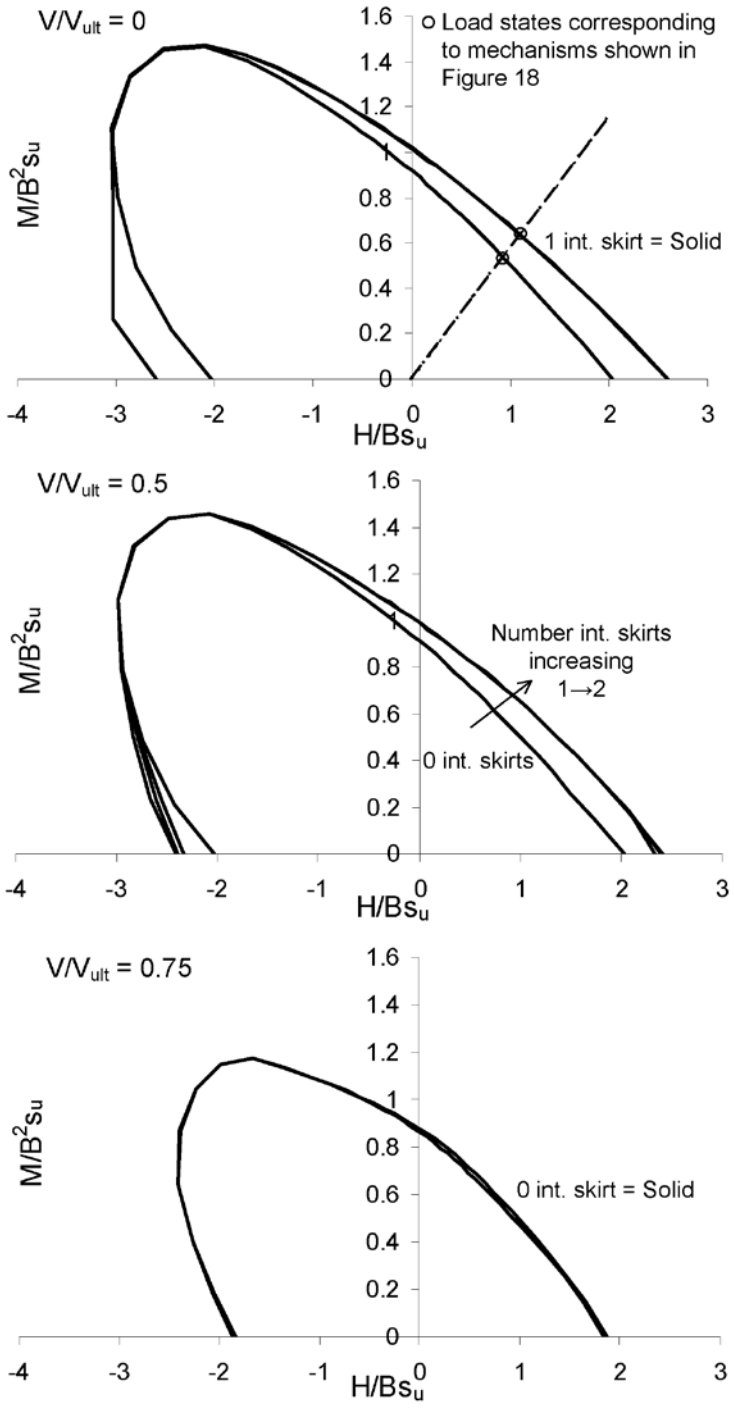
V/V_ult = 0
o Load states corresponding to mechanisms shown in Figure 18
1 int. skirt = Solid
M/B²s_u
H/Bs_u
V/V_ult = 0.5
Number int. skirts increasing 1→2
0 int. skirts
M/B²s_u
H/Bs_u
V/V_ult = 0.75
0 int. skirt = Solid
M/B²s_u
H/Bs_u

Figure 14

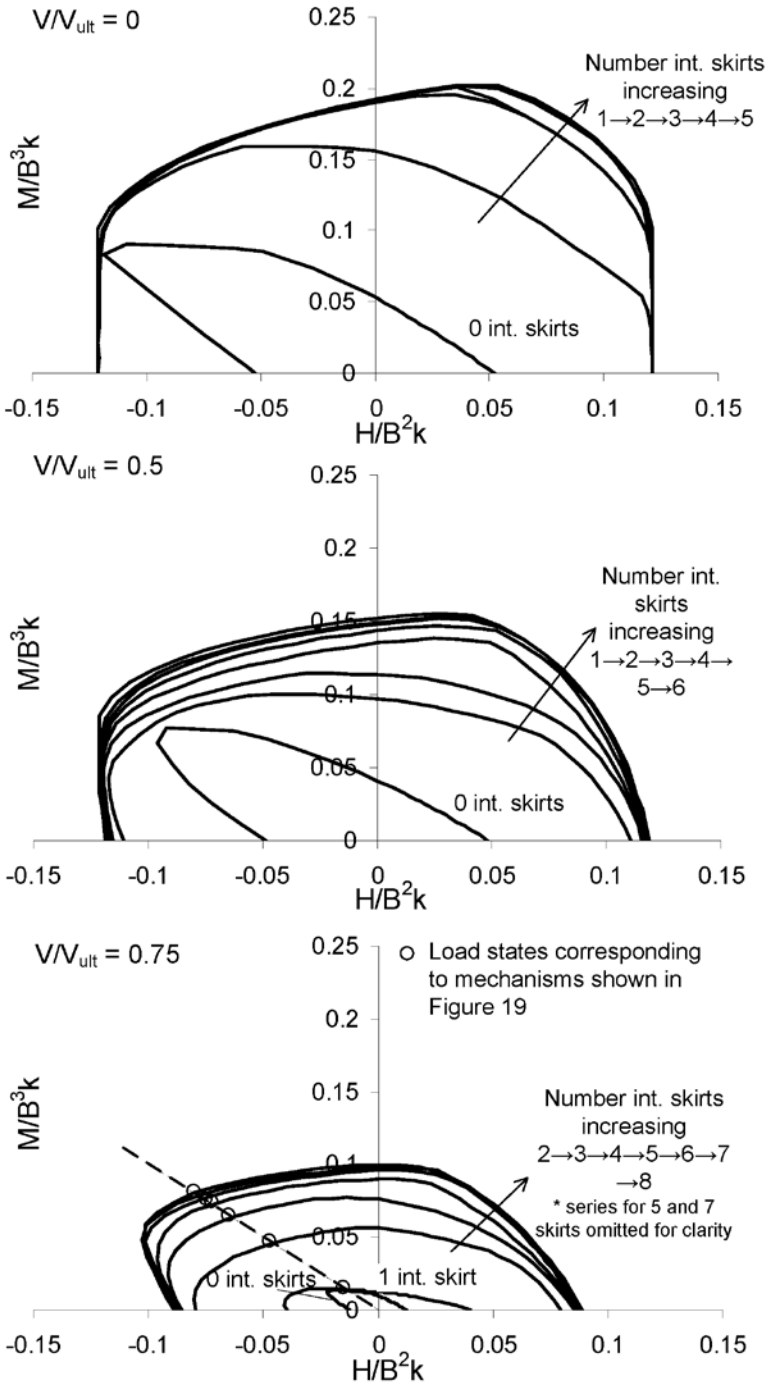
V/V_ult = 0
Number int. skirts increasing 1→2→3→4→5
0 int. skirts
M/B^3k
H/B^2k
V/V_ult = 0.5
Number int. skirts increasing 1→2→3→4→5→6
0 int. skirts
M/B^3k
H/B^2k
V/V_ult = 0.75
Load states corresponding to mechanisms shown in Figure 19
Number int. skirts increasing 2→3→4→5→6→7→8
* series for 5 and 7 skirts omitted for clarity
0 int. skirts
1 int. skirt
M/B^3k
H/B^2k

Figure 15

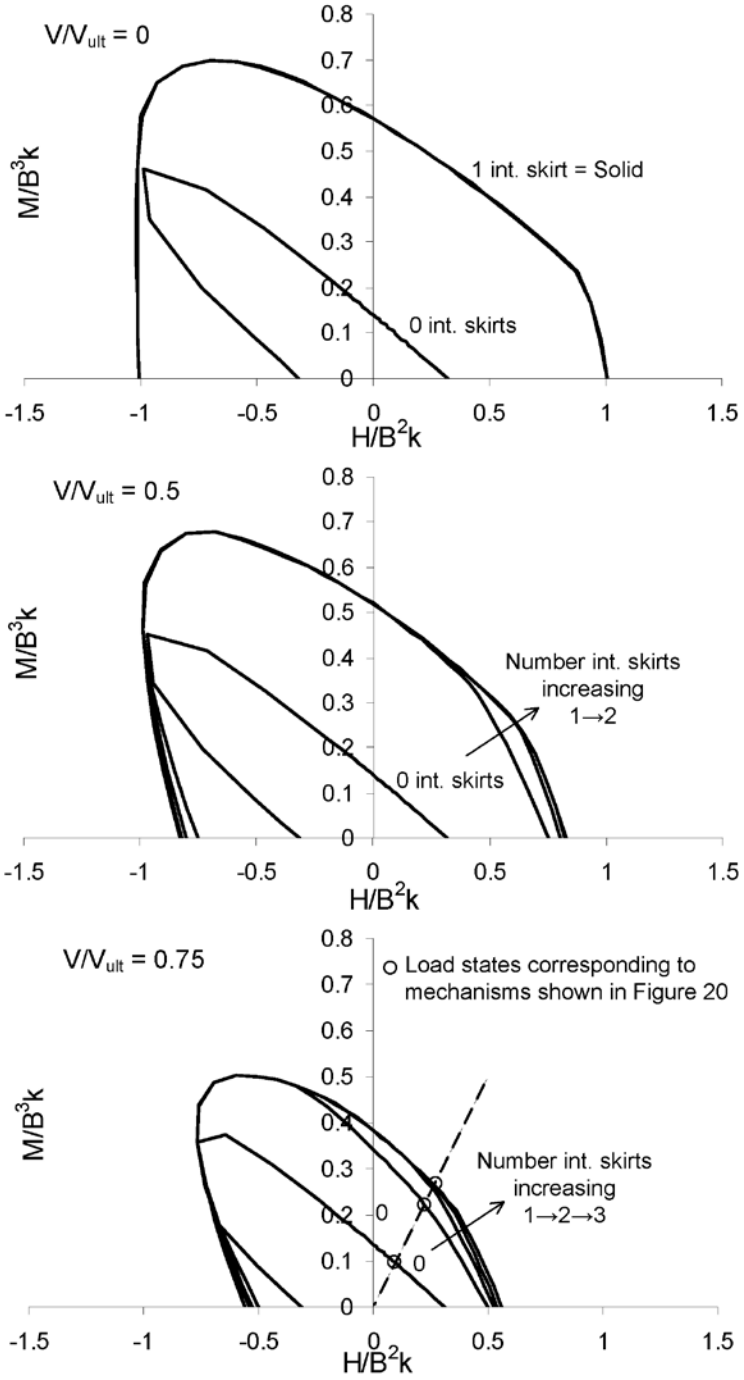
V/V_ult = 0
1 int. skirt = Solid
0 int. skirts
M/B^3k
H/B^2k
V/V_ult = 0.5
Number int. skirts increasing 1→2
0 int. skirts
V/V_ult = 0.75
Load states corresponding to mechanisms shown in Figure 20
Number int. skirts increasing 1→2→3

Figure 16

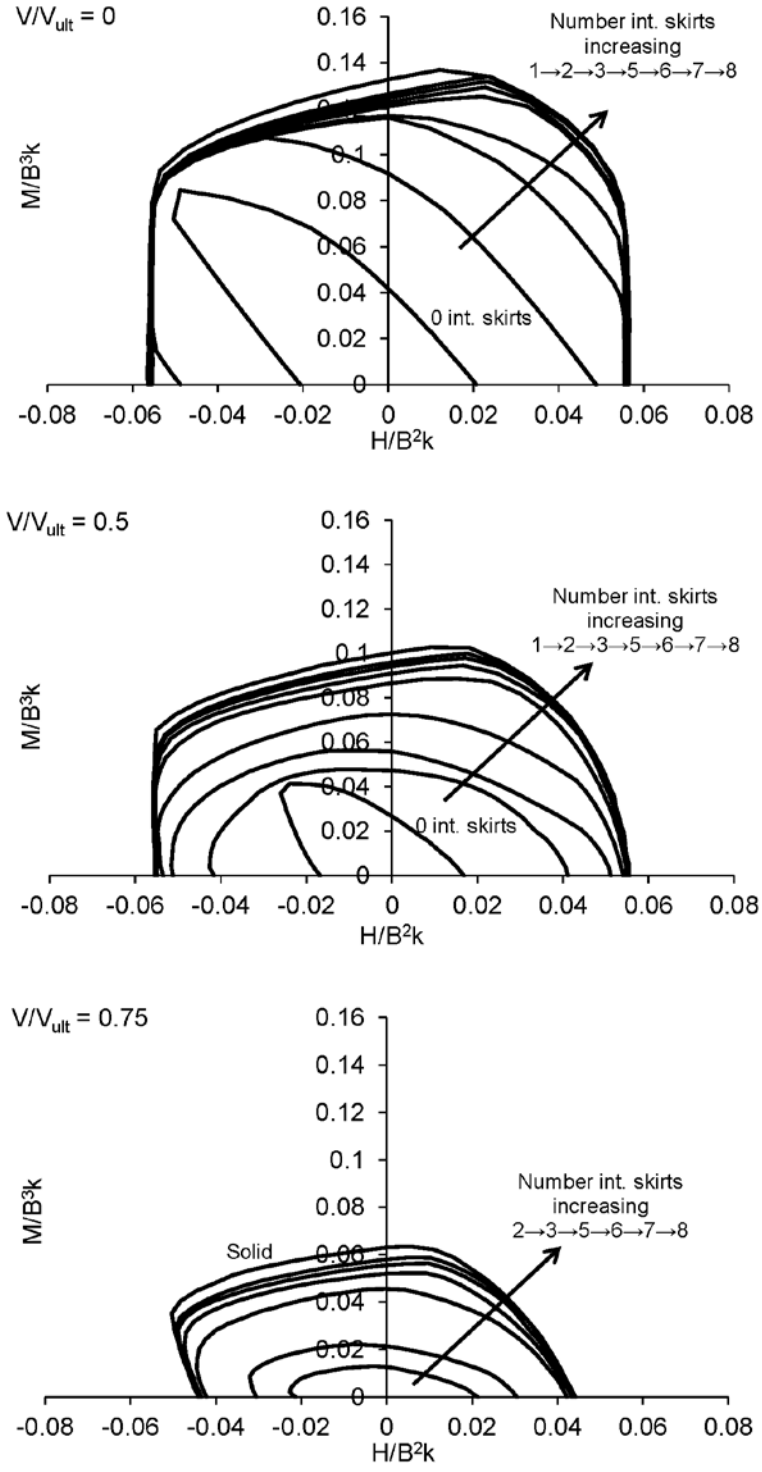
V/V_ult = 0
Number int. skirts increasing 1→2→3→5→6→7→8
0 int. skirts
M/B³k
H/B²k
V/V_ult = 0.5
Number int. skirts increasing 1→2→3→5→6→7→8
0 int. skirts
M/B³k
H/B²k
V/V_ult = 0.75
Number int. skirts increasing 2→3→5→6→7→8
Solid
M/B³k
H/B²k

Figure 17

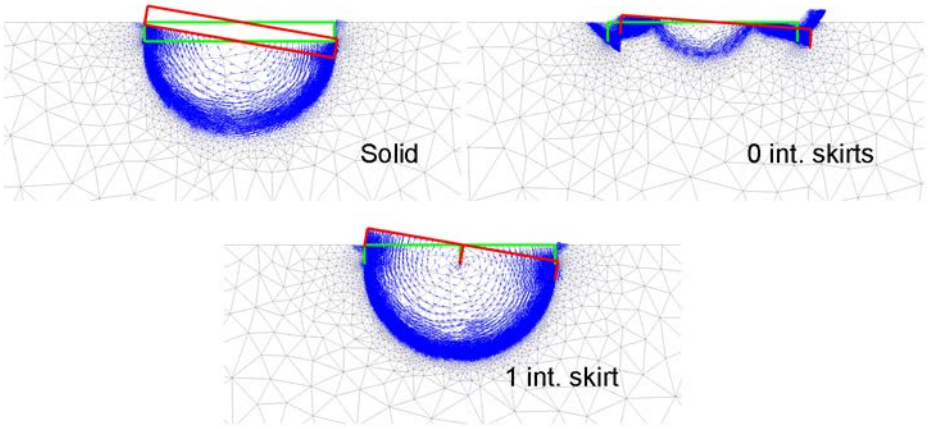

Figure 18

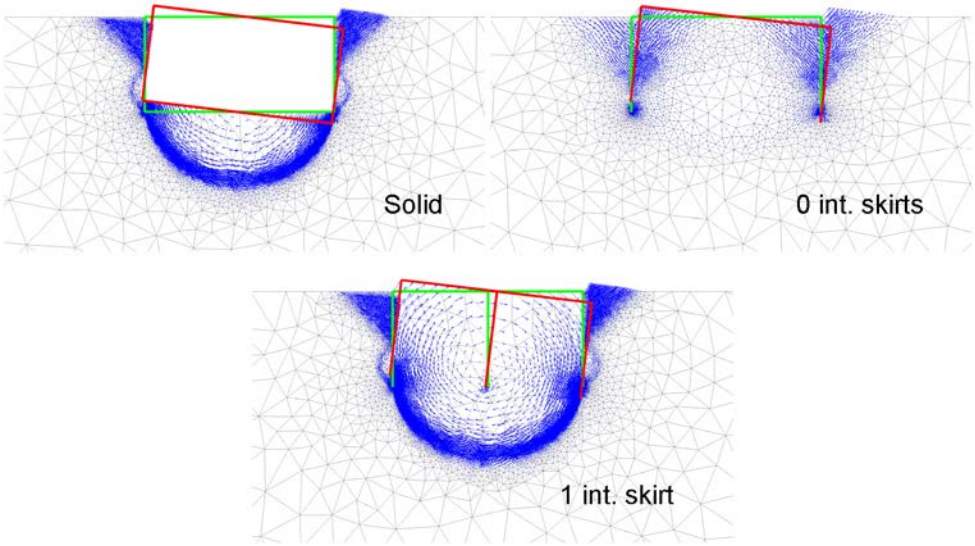

Figure 19

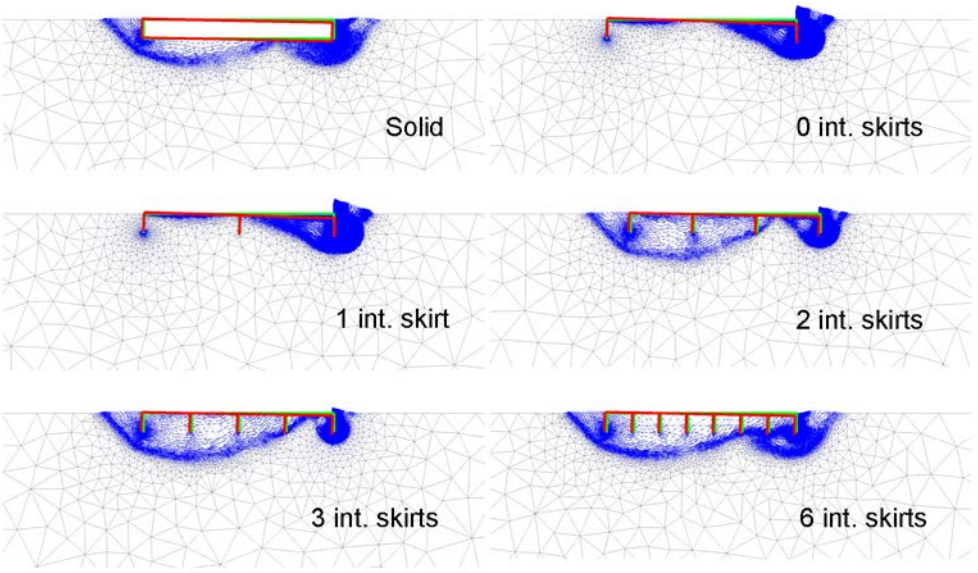

Figure 20

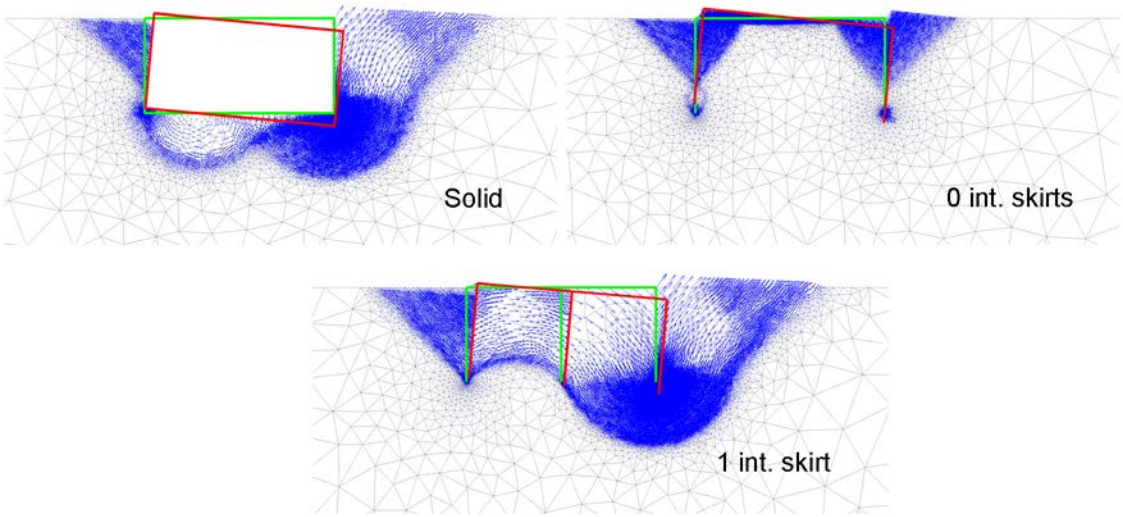

Figure 21

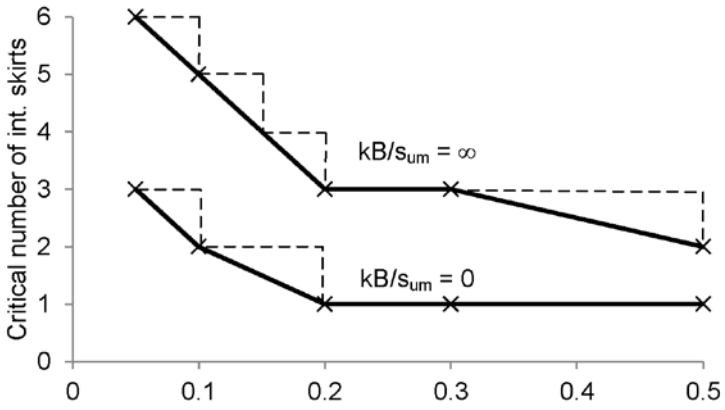

Figure 22

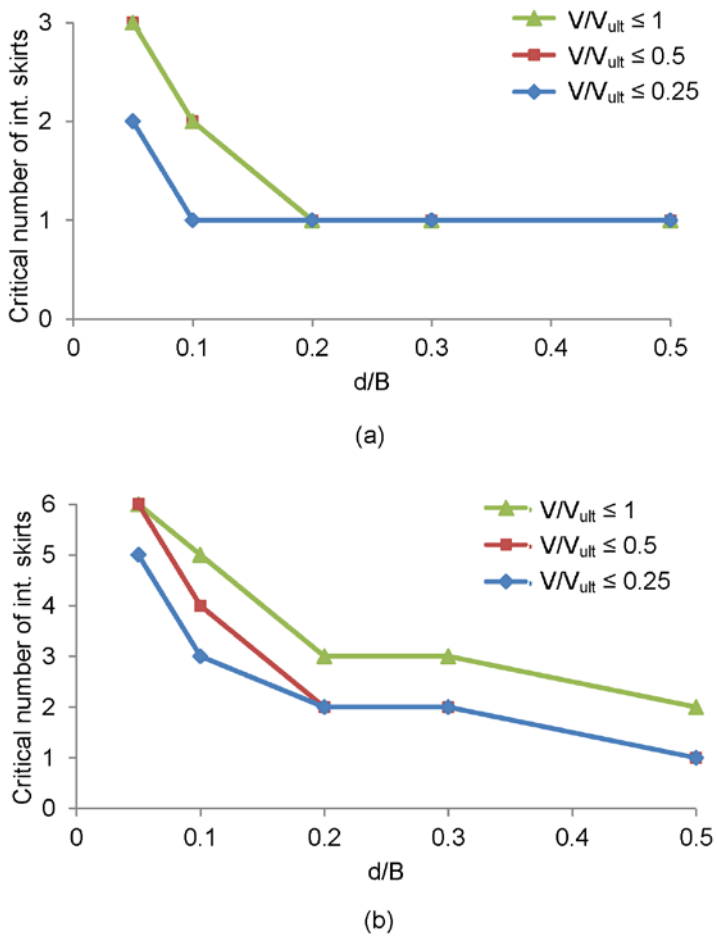

Figure 23